DSN Telecommunications Link
Design Handbook

203, Rev. C
Sequential Ranging

Released October 31, 2009

Prepared by:

P. W. Kinman Date

Approved by:

T. T. Pham Date
DSN Chief System Engineer

Released by:

Signature on File at DSN Library 10/31/2009
DSN Document Release Date

Change Log

Rev	Issue Date	Affected Paragraphs	Change Summary
Initial	1/15/2001	All	All
A	2/20/2006	Many	Revised to incorporate changes resulting from improvements in sequential ranging implementation.
B	4/2/2007	2.6	Added new paragraph at end of 2.6 providing recommended range for P_r/N_0
C	10/31/2009	Page 5, 31, 40, A1 & A2	Removed references of the 26-m subnet stations for they have been decommissioned. Made editorial changes. Replaced Reference 2.

Note to Readers

There are two sets of document histories in the 810-005 document that are reflected in the header at the top of the page. First, the entire document is periodically released as a revision when major changes affect a majority of the modules. For example, this module is part of 810-005, Revision E. Second, the individual modules also change, starting as an initial issue that has no revision letter. When a module is changed, a change letter is appended to the module number on the second line of the header and a summary of the changes is entered in the module's change log.

Contents

Illustrations

Tables

1 Introduction

1.1 Purpose

This module describes capabilities and expected performance of the DSN when supporting sequential ranging. These capabilities are available at all DSN stations.

1.2 Scope

The material contained in this module covers the sequential ranging system that may be utilized by both near-Earth and deep space missions. This document describes those parameters and operational considerations that are independent of the particular antenna being used to provide the telecommunications link. For antenna-dependent parameters, refer to the appropriate telecommunications interface module, modules 101, 102, 103, and 104 of this handbook. Another type of ranging, pseudo-noise ranging, is described in module 214.

An overview of the ranging system is given in Paragraph 2.1. The signal structure is described in Paragraph 2.2. The parameters to be specified for ranging operations are identified in Paragraph 2.3. The distribution of link power is characterized in Paragraph 2.4. The spectrum of an uplink carrier modulated by a sequential ranging signal is discussed in Paragraph 2.5. The performance of sequential ranging is summarized in Paragraph 2.6. Calibrations are discussed in Paragraph 2.7. Error contributions of the ground instrumentation are estimated in Paragraph 2.8.

2 General Information

The DSN ranging system measures the round-trip phase delay of a ranging signal sent from an uplink Deep Space Station (DSS) to a spacecraft and back to a downlink DSS. In the most common configuration, known as two-way ranging, the uplink and downlink stations are the same, and the measured two-way phase delay permits the determination of the round-trip light time (RTLT) between the DSS and spacecraft.

For some outer planet missions, the light time between Earth and the spacecraft is large enough that a one-station range measurement (two-way ranging) is not possible. In such a case, the more general configuration, in which the uplink and downlink stations are different, may be used. This is known as three-way ranging.

Deep-space range measurements may be made using either sequential ranging or pseudo-noise (PN) ranging signals. Both signaling techniques are employed in the same set of stations using the same instrumentation and provide similar results. However, there are performance differences between these two techniques (Reference 1). Sequential ranging is the subject of this module. PN ranging is described in module 214.

A range measurement may be made with a constant uplink carrier frequency or when the transmitted uplink carrier frequency is time varying. For some missions, it is desirable

to anticipate the uplink Doppler effect and to transmit an uplink carrier whose frequency varies in such a way that the uplink carrier arrives at the spacecraft with minimal offset from channel center. This is called uplink Doppler compensation and has the advantage of reducing the stress on the carrier tracking loop in the spacecraft receiver. The DSN ranging system accommodates both a time-varying and a constant transmitted uplink frequency. In the interpretation of the data, however, the case of a time-varying transmitted uplink frequency requires more mathematics. In particular, it is necessary to know and to account for the time history of the transmitted uplink frequency from the start of ranging sequence at the uplink station to the end of the received ranging sequence at the downlink station (Reference 2).

There is an ambiguity associated with range measurement as there is with any measurement of phase delay. The user of the measured data must resolve the ambiguity using *a priori* (pre-measurement) estimates. The time delay and the actual range to the spacecraft may be inferred from the measured phase delay.

Range data are delivered to users in Range Units (RU) modulo the ambiguity resolution capability that was established during system initialization. The RU is defined, for historical reasons related to hardware design, as follows. With an S-band uplink, 1 RU of phase is defined as two cycles of the uplink carrier frequency. With an X-band uplink, 1 RU of phase is defined as two cycles of a hypothetical sinewave with frequency equal to $221/749$ times that of the uplink carrier frequency. (The factor $221/749$ equals the ratio of the channel-center carrier frequency for an S-band uplink to that for an X-band uplink with the same channel number.) Two cycles of an S-band uplink carrier (or two cycles of a sinewave having a frequency equal to the X-band uplink carrier frequency multiplied by $221/749$) have a duration of approximately 0.94 ns. Therefore, 1 RU of phase delay is roughly equivalent to 1 ns of time delay (regardless of whether the uplink is in the S or X band).

In general, an accurate translation of the observed phase delay to a time delay is a complicated calculation involving the time history of the transmitted uplink frequency (Reference 2). Often, however, ranging is done with a constant transmitted frequency; in this case, the translation is easily accomplished:

$$\text{Unresolved Time Delay} = \begin{cases} \dfrac{2 \times RU}{f_S}, & \text{S - band uplink} \\ \dfrac{749}{221} \cdot \dfrac{2 \times RU}{f_X}, & \text{X - band uplink} \end{cases} \tag{1}$$

where RU is the reported number of range units and f_S is the frequency of the S-band uplink carrier or f_X is the frequency of the X-band uplink carrier. It is important to recognize that Equation (1) gives the *unresolved* time delay, equal to the two-way time delay modulo T_L seconds, where T_L is the period of the last ambiguity-resolving component. When the unresolved time delay of Equation (1) is multiplied by $c/2$, where c (299,792.50 km/s) is the speed of electromagnetic waves in vacuum, the result is the unresolved range, which equals the range modulo $cT_L/2$. For example, if an X-band uplink of 7,160 MHz is being used and the range observable is 6,500,000 RU, then the unresolved two-way time delay is 6,153,467 ns and the

unresolved range is 922,381.6 m. It is perhaps instructive to work this example backwards as well. For a transmitted uplink carrier frequency of 7,160 MHz and with $L = 24$, T_L is 1.01649766953 s and $cT_L/2$ is 152,369,188.80 m. If the range is 152,370,111,177.37 m, then the range modulo $cT_L/2$ will be 922,381.6 m and the range observable will be 6,500,000 RU.

2.1 System Description

The architecture for the DSN ranging system is shown in Figure 1. It consists of a front-end portion, an Uplink Subsystem (UPL), and a Downlink Telemetry and Tracking Subsystem (DTT). The front-end portion includes the microwave components, including a low-noise amplifier (LNA), the transmitter, and the antenna. The UPL includes the Uplink Ranging Assembly (URA), the exciter, and their controller, referred to as the Uplink Processor Assembly (UPA). The DTT includes the RF-to-IF Downconverter (RID) located on the antenna, the IF-to-Digital Converter (IDC), the Receiver and Ranging Processor (RRP) and the Downlink Channel Controller (DCC). References 3 and 4 offer more detail.

The URA uplink ranging function is controlled by the UPA. The RRP downlink ranging function is controlled by the DCC. Each measures the range phase and sends the measurements to the Tracking Data Delivery Subsystem (TDDS) via the Reliable Network Service (RNS). The URA generates the uplink ranging signal and measures its phase before passing it to the exciter. The signal is phase-modulated onto the carrier by the exciter and, after being amplified to a suitable level by the transmitter, is forwarded to the spacecraft. The spacecraft coherently transponds the signal, sending it back to the DSN receiver.

The amplified downlink signal from the antenna is downconverted by the RID (located on the antenna) and fed to an intermediate frequency (IF) distribution assembly in the control room. The IF is fed to one or more Downlink Channel Processing Cabinets (DCPC) as required. Each DCPC is equipped with a single channel, which includes a single IDC and RRP. For a spacecraft that requires ranging on multiple downlinks (for example, S-band and X-band), multiple DCPCs will be assigned to that antenna.

After processing, the downlink range phase data are delivered to the TDDS by the Downlink Channel Controller (DCC), via the station RNS and a similar function at JPL. The TDDS combines the uplink and downlink phase information to produce a measure of the two-way phase delay, which is called range data. (This is a misnomer, since the data have units of phase, not distance.) The TDDS then formats the range data and passes it, along with the uplink and downlink information, to the Navigation subsystem (NAV). Subsequently, the NAV provides the ranging data to projects.

Three-way ranging is accomplished in essentially the same way as two-way ranging, except that there are two stations. The UPL, transmitter, and antenna of one DSS are used to transmit an uplink carrier modulated with a ranging signal. The uplink range phase is recorded at that station. At a second DSS, the antenna, LNA and DTT receive the downlink from the spacecraft and record the downlink range phase.

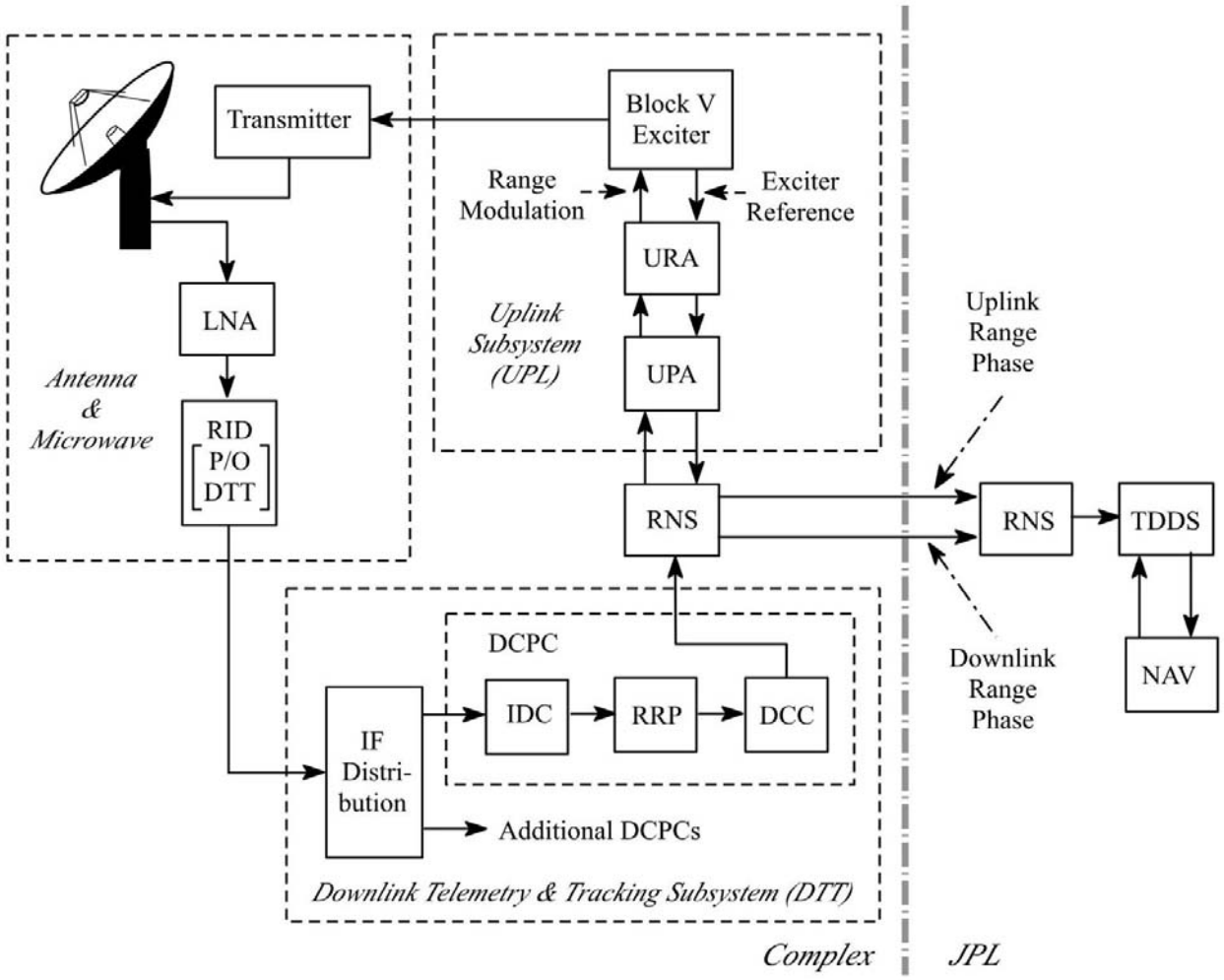

Figure 1. The DSN Ranging System Architecture

2.2 Sequential Ranging Signal Structure

The sequential ranging signal is a sequence of periodic signals. These periodic signals are all coherently related to each other and to the uplink carrier. The basis for these periodic ranging signals is a table of well-defined range components.

2.2.1 Range Components

The range components are periodic signals. Each component is assigned a number. A larger number represents a component with a smaller frequency (but a larger period). The components that are used in ranging are assigned the numbers 4 through 24 and are ordered according to these component numbers. The frequency f_0 of the theoretical component 0 is related to the uplink carrier frequency by

$$f_0 = \begin{cases} 2^{-7} \times f_S , & \text{S - band uplink} \\ 2^{-7} \times \dfrac{221}{749} \times f_X , & \text{X - band uplink} \end{cases} \tag{2}$$

where f_S is the frequency of the S-band uplink carrier or f_X is the frequency of the X-band uplink carrier. The frequency f_n of component n is related to f_0 by

$$f_n = 2^{-n} \times f_0 \tag{3}$$

Since the component frequencies are related to the uplink carrier frequency, the exact values of the component frequencies depend on the channel assignment and any uplink Doppler compensation that may be present. An example table of the transmitted range component frequencies is given in Table 1 for channel assignment 18, assuming the transmitted uplink carrier is at its nominal channel frequency (no uplink Doppler compensation). The frequencies of Table 1 are rounded-off to the nearest millihertz. (In a typical measurement, the component frequencies are known to a better accuracy than 1 mHz. The intent of Table 1 is to give the reader a general idea of the component frequencies and how they vary with component number.) Even though Table 1 represents a particular case (nominal Channel 18), there are discernable features of this table that are also present in any table of range component frequencies. The frequency of component 4 is always approximately 1 MHz, and it is often called the “1 MHz component”. The frequency of components 5 through 24 is exactly half of their immediate predecessor.

There is an ambiguity whenever a periodic signal is used to measure signal delay. The phase delay consists, in principle, of an integer number of cycles plus some fraction of a cycle. If only one periodic signal of frequency f_n is used in the measurement, only the fractional part of the phase delay (a fraction of one cycle) can be measured. The integer number of cycles in the delay cannot be known from the measurement itself. However, *a priori* knowledge of the approximate value of the delay may provide that information. The successful resolution of the ambiguity requires that the *a priori* estimate of the delay be correct to within 1 cycle of phase. In time units, the *a priori* estimate of the delay must be correct to within 1 period $\left(1/f_n\right)$.

Table 1. Range Components for Channel 18 (Nominal)

Component Number	Frequency (Hz)	Ambiguity-Resolving Capability (km)
4	1,032,556.981	0.1452
5	516,278.490	0.2903
6	258,139.245	0.5807
7	129,069.623	1.1614
8	64,534.811	2.3227

9	32,267.406	4.6454
10	16,133.703	9.2909
11	80,66.851	18.5818
12	4,033.426	37.1635
13	2,016.713	74.3270
14	1,008.356	148.6540
15	504.178	297.3081
16	252.089	594.6161
17	126.045	1,189.2323
18	63.022	2,378.4645
19	31.511	4,756.9291
20	15.756	9,513.8581
21	7.878	19,027.7163
22	3.939	38,055.4326
23	1.969	76,110.8651
24	0.985	152,221.7303

Considering that the speed of an electromagnetic wave in vacuum is 299,792.50 km/s (c) and that the delay measurement is two-way, the *a priori* estimate of the range must be correct to within $c/(2 f_n)$ if the ambiguity is to be resolved. This is the number entered in the third column of Table 1.

2.2.2 Range Clock

The first periodic signal in the ranging sequence is called the range clock. Any of components 4 through 10 may be selected by the user for the range clock. If the range clock is component 4, 5 or 6, then it is a sinewave. (The spectrum of a modulated carrier is narrower when the modulating signal is sinewave, rather than squarewave, for a given modulating frequency. Good spectrum management therefore requires that the higher-frequency range clocks, having component numbers 6 or less, be sinewave.) If the range clock is component 7, 8, 9 or 10, then the user may choose for the range clock to be either a sinewave or a squarewave. With component k as the range clock, the frequency f_k of the range clock is

$$f_k = \begin{cases} 2^{-7-k} \times f_S\,, & \text{S - band uplink} \\ 2^{-7-k} \times \dfrac{221}{749} \times f_X\,, & \text{X - band uplink} \end{cases} \tag{4}$$

This equation is consistent with Equations (2) and (3).

2.2.3 Ranging Sequence

The ranging signal consists of a sequence of range components. The first is the range clock – one of the range components 4 through 10. The second is the component having a component number equal to one plus that of the range clock. The third is the component having a component number equal to two plus that of the range clock, and so forth. For example, if the range clock is component 4, then the sequence is 4, 5, 6… .

All range components in a ranging sequence except the range clock are known as ambiguity-resolving components. The number of ambiguity-resolving components that should be used in the ranging sequence for any particular range measurement is determined by the required ambiguity-resolving capability for that measurement. The range components always occur sequentially, in order of increasing component number, without skipping any, from the range clock to the last ambiguity-resolving component.

In any given measurement, some ambiguity-resolving components may be multiplied by a higher-frequency component; this multiplication is called chopping. The purpose of chopping is to enforce spectral isolation between the ranging signal and command on the uplink and between the ranging signal and telemetry on the downlink. The effect of the chopping is to modulate the lower frequency range components onto a ranging subcarrier. This ranging subcarrier is called the chop component. The chop component is of the same type (sinewave or squarewave) as the range clock. Typically, the chop component is the range clock but it can be any of the components from 4 through 10. The component that is multiplied by the chop component is always squarewave. Figure 2 shows an example of (squarewave) component 6 multiplied by (sinewave) component 4. (In this case, the chop component has a frequency four times that of the squarewave component, so there are two cycles of the chop component for each

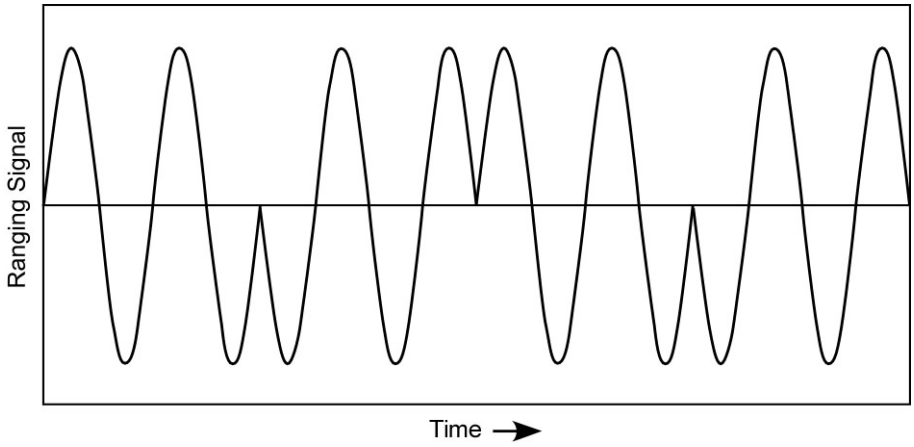

Figure 2. Squarewave Component 6 Multiplied by Sinewave Component 4

half-cycle of the squarewave.) The user specifies at which point in the sequence the chopping should begin; all components after this point are multiplied by the chop component. The user also specifies the chop component. This chop component remains the same for the duration of the range measurement session.

Following the range clock, all subsequent components that are not multiplied by the chop component are of the same type (either sinewave or squarewave) as the range clock. The chop component, which is one of these, is also of the same type as the range clock. Typically, the range clock is the chop component. Here is an example sequence:

1. sinewave component 4 (range clock)
2. sinewave component 5
3. sinewave component 6
4. squarewave component 7 multiplied by sinewave component 4
5. squarewave component 8 multiplied by sinewave component 4

etc.

In this example sequence, the range clock is the chop component.

The purpose of ranging with a sequence is to get the advantages of both high-frequency and low-frequency range components. The accuracy of a range measurement improves when a higher-frequency range clock is used (see Paragraph 2.6). All components that follow the range clock resolve the phase ambiguity. The ambiguity-resolving capability of a ranging sequence equals the ambiguity-resolving capability of the lowest-frequency range component (see Table 1).

2.2.4 Sequence Timing

Three parameters control the timing of the transmitted sequence: the transmit time (XMIT), the integration time T_1 that is to be used for the range clock, and the integration time T_2 that is used to be used for each of the ambiguity-resolving components. XMIT is always selected to fall on an integer-second epoch, as established by the station clock. Each of the integration times T_1 and T_2 is an integer number of seconds.

2.2.4.1 Timing at the Exciter

The actual start time of the ranging sequence at the exciter, which is also the start time of the range clock, is 1 s before XMIT. The purpose of this slightly early start is to increase the probability that the range clock integration at the receiver does not begin before the range clock arrives at the receiver. Once the ranging sequence has started, the phase of the modulating signal is continuous throughout the ranging sequence, including at the transitions from one component to the next. This is essential for the correct resolution of the phase ambiguity.

The range clock persists from the (XMIT –1 s) epoch up through the (XMIT + T_1 + 1 s) epoch. The transition from the range clock to the first ambiguity-resolving component occurs sometime within the 1-s interval that immediately follows the (XMIT + T_1 + 1 s) epoch at a point where phase continuity can be maintained. Hence, the range clock is present for T_1 + 2 s plus a fraction of another second.

Once the first ambiguity-resolving component has started, it persists through the (XMIT + T_1 + T_2 + 2 s) epoch. The transition to the next ambiguity-resolving component occurs sometime within the 1-s interval that immediately follows the (XMIT + T_1 + T_2 + 2 s) epoch at a point where phase continuity can be maintained. Hence, the first ambiguity-resolving component has a duration of at least T_2. The actual duration is typically about T_2 + 1 s lasting from a fraction of a second before the (XMIT + T_1 + 2 s) epoch until a fraction of a second after the (XMIT + T_1 + T_2 + 2 s) epoch but there can be no assurance that the duration will exceed T_2.

In general, the transition to the *n*-th ambiguity-resolving component occurs a fraction of a second before the $\left\{\text{XMIT} + T_1 + 2\text{ s} + \left(n-1\right)\left(T_2 + 1\text{ s}\right)\right\}$ epoch. The duration of the *n*-th ambiguity-resolving component is typically about T_2 + 1 s, but there can be no assurance that the duration will exceed T_2.

Figure 3 shows an example of the sequence timing. In this example, the range clock is component 4 (C4) and the last component is 9 (C9). The range clock begins 1 s before XMIT and continues for an additional T_1 seconds (for the nominal measurement) plus 1 s (as a margin for error). During the next second, there is a transition from the range clock to component 5 (C5). The transition itself occurs instantaneously at a point where phase continuity can be maintained but there is no guarantee of when within this second the actual transition occurs. There is another transition second following the planned T_2-s period for C5. The pattern

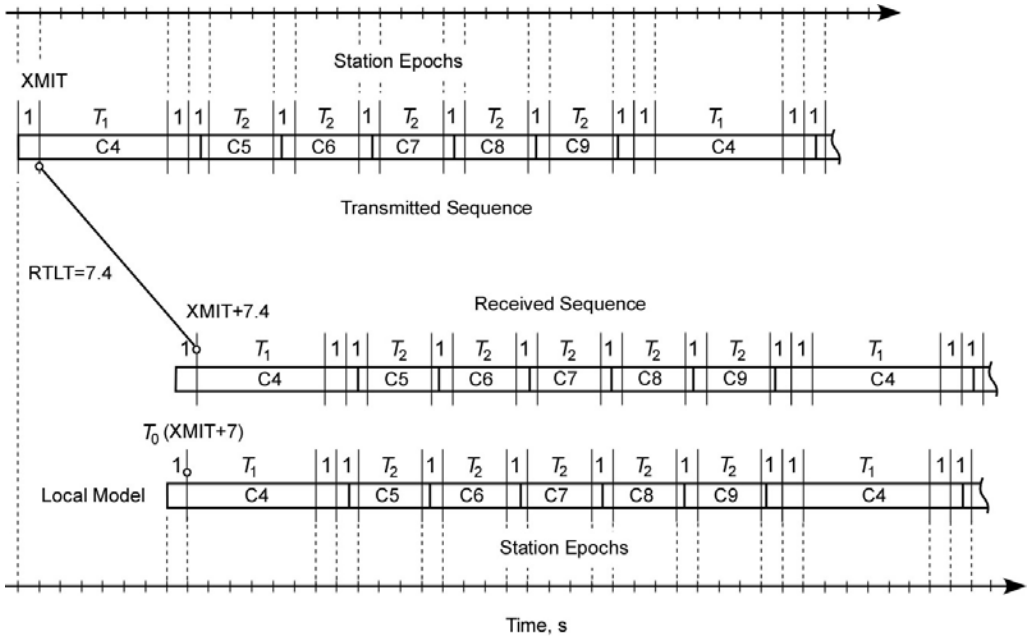

Figure 3. Example Timing Diagram (T_1 = 6 s, T_2 = 3 s, RTLT = 7.4 s)

established by C5 is repeated for components 6 through 9 (C6 through C9). Following a transition second that accommodates the transition from C9 back to C4 (in preparation for a second range measurement), the range clock is transmitted for 1 sec (as a margin for error) plus T_1 seconds (for the nominal measurement), and so forth.

2.2.4.2 Timing at the Receiver

The estimated RTLT is an input parameter to the ranging receiver. This estimate is rounded-off to the nearest integer second within the DTT. The rounded-off, estimated RTLT is added to XMIT to get the start time T_0 of the range clock integration. The range clock integration extends from the T_0 epoch to the $T_0 + T_1$ epoch. The error introduced to T_0 by round-off is no larger than 0.5 s. Therefore, T_0 is different from XMIT + RTLT by less than 1 s. That is why the range clock at the exciter begins 1 s before the specified sequence start time and ends $T_1 + 1$ s after the specified start time. The 1-s padding at the start and at the end of the range clock interval ensures that the range clock is present at the receiver during the entire range clock integration provided the estimated RTLT was correct to within 0.5 s.

The integration for the first ambiguity-resolving component begins at the $T_0 + T_1$ + 2 s) epoch. Hence, there is 2-sec interval that separates the range clock integration from that for the first ambiguity-resolving component.

In general, the integration for the *n*-th ambiguity-resolving component begins at the $\left\{T_0 + T_1 + 2\text{ s} + \left(n-1\right)\left(T_2 + 1\text{ s}\right)\right\}$ epoch. There is a 1-second interval that separates the integrations of any two ambiguity-resolving components.

The actual RTLT in the Figure 3 example is 7.4 s. Assuming this is also the estimate, the value is rounded-off to 7 s within the DTT and T_0 is less than XMIT + RTLT by 0.4 s. In this case, the local model is 0.4 s in advance of the received sequence. The timing of the component integrations is determined by this local model so all integrations begin 0.4 sec early.

T_0 does not, in general, exactly equal XMIT + RTLT; therefore, the integration of each ambiguity-resolving component in a range measurement may begin slightly before the component to be integrated is received or the component being integrated may end slightly before the end of the integration time. In such cases, the effective integration time for each ambiguity-resolving component is slightly less than the design value, T_2. The difference between the design value and the effective value of T_2 is typically a fraction of a second. Normally, this is not a problem. However, the degradation in performance may be noticeable if the design value T_2 is only 1 or 2 seconds (see Paragraph 2.6.4.1). As mentioned previously, this alignment problem does not affect the range clock integration as long as the estimated RTLT is correct to within 0.5 s, owing to the 1-second padding at the start and the end of the range clock interval.

2.2.4.3 Cycle Time

Range measurements typically are done serially during a tracking pass. For each range measurement, there is a ranging sequence of the type described above (a range clock followed by a set of ambiguity-resolving components). When the ranging sequence associated with one range measurement ends, another ranging sequence with exactly the same signal structure begins immediately. The cycle time is the repetition period of the range measurements and is given by

$$\text{Cycle Time } = T_1 + 3 + \left(L - C\right)\left(T_2 + 1\right), \text{ s} \tag{5}$$

where L is the range component number of the last ambiguity-resolving component and C is the range component number of the range clock. In light of the previous discussion of sequence timing, Equation (5) can be understood as follows. There is a period of time, T_1 + 2 s, during which the range clock is transmitted, followed by a 1-second interval that contains the transition from the range clock to the first ambiguity-resolving component. This is the T_1 + 3 appearing in Equation (5). There are $L - C$ ambiguity-resolving components. Each of these components has a duration T_2 and a 1-second interval containing the transition to the next component.

The last component L should be chosen carefully if it is desirable to maximize the number of range data points in a tracking pass. For any given *a priori* range ambiguity, there is a minimum L that will resolve the ambiguity (see Table 1). Choosing an L larger than this will reduce the number of range data points that can be obtained in a tracking pass. Table 2 shows the number of range points that can be obtained per hour as a function of L using component 4 as

Table 2. Range Points per Hour for Representative Values of T_2; C = 4 and T_1 = 100 s

L	Range Points per Hour	
	T_2 = 5 s	T_2 = 20 s
12	23.8	13.3
13	22.9	12.3
14	22.1	11.5
15	21.3	10.8
16	20.6	10.1
17	19.9	9.6
18	19.3	9.1
19	18.7	8.6
20	18.1	8.2
21	17.6	7.8
22	17.1	7.5
23	16.6	7.2
24	16.1	6.9

the range clock, T_1 = 100 s and T_2 values of 5 s and 20 s. Only whole cycles are valid and the numbers in the table need to be multiplied by the pass length and truncated to predict the number of cycles for a tracking pass.

2.3 Parameters Specified for Ranging Operations

The following paragraphs present the parameters that are required in ranging operations.

2.3.1 Ranging Sequence Parameters

The ranging sequence is established by specifying the range clock component number, the last component number, the chop component number, the component number at which chopping begins, and the integration times, T_1 and T_2.

The range clock component number determines the approximate frequency of the range clock. The exact frequency of the range clock is set by its relation to the uplink carrier frequency (see Paragraph 2.2.2). The highest frequency that can be used for the range clock is

that corresponding to range component 4. Since better range measurement accuracy is achieved with a higher-frequency range clock (see Paragraph 2.6), range component 4 is typically selected for the range clock. However, any of components 4 through 10 may be selected by the user for the range clock. If the range clock is component 4, 5 or 6, then it is a sinewave. If the range clock is component 7, 8, 9 or 10, then the user may choose for the range clock to be either a sinewave or a squarewave.

The last component number determines the ambiguity-resolving capability of the ranging sequence. Therefore, the proper selection of this number depends on *a priori* knowledge of the range. The approximate ambiguity-resolving capability of the different range components is given in Table 1. The exact ambiguity-resolving capability depends on the uplink frequency.

The purpose of chopping is to enforce spectral isolation between the ranging sequence and the command signal on the uplink and between the ranging sequence and the telemetry signal on the downlink. Selection of the chop component and the component at which chopping begins should be made with this in mind.

There is a fundamental trade-off in the selection of the integration times T_1 and T_2. On the one hand, a large T_1 decreases the range measurement error due to thermal noise and a large T_2 increases the probability of range acquisition (see Paragraph 2.6). On the other hand, large values for T_1 and T_2 increase the cycle time (see Paragraph 2.2.4.3), decreasing the number of range measurements that can be made in a tracking pass. The selection of these integration times will depend on the available P_R/N_0 (see Paragraph 2.6).

2.3.2 Correlation Type

Either a sinewave or a squarewave may be used at the receiver as the local model of the range clock for the purpose of correlation. Normally, the user will select a local model that matches the form of the actual range clock. That is to say, when the range clock is sinewave, the user will normally select sinewave correlation. When the range clock is squarewave (which is permissible if the range clock component number is 7, 8, 9, or 10), the user will normally select squarewave correlation. A small degradation in performance results if a local model is selected that does not match the form of the actual range clock.

2.3.3 Modulation Indices

Both the uplink and the downlink ranging modulation indices affect range measurement performance.

2.3.3.1 Uplink Ranging Modulation Index

The uplink ranging modulation index is chosen to get a suitable distribution of power among the ranging and command sidebands and the residual carrier on the uplink (see Paragraph 2.4.1). The uplink ranging modulation index also affects the distribution of power on the downlink carrier.

2.3.3.2 Downlink Ranging Modulation Index

The downlink ranging modulation index is set in the spacecraft transponder either during manufacture or by spacecraft command. It is usually kept constant, independent of both the uplink signal level and the signal-to-noise ratio in the ranging channel, by automatic gain control in the ranging channel. In a typical deep-space ranging scenario, there is more noise power than signal power in the ranging channel. Therefore, the effective ranging signal modulation index is quite different from the index used to modulate the contents of the ranging channel (signal plus noise) on the downlink carrier.

2.3.4 Probability of Acquisition Tolerance

The Probability of Acquisition (P_{acq}) Tolerance is used to set the acceptable limit on the probability of range acquisition. P_{acq} is an estimate of the probability of range acquisition expressed as a percentage, based on the measured P_R/N_0 (see Paragraph 2.6).

It may be set anywhere in the range of 0.0% to 100.0%. As an example, if tolerance is set to 0.0%, all range acquisitions made while the downlink carrier is in lock are declared valid. On the opposite extreme, if the tolerance is set to 100.0%, all range acquisitions will be declared invalid. A typical value set for tolerance is 99%. This value will flag acquisitions that have a 99% or better chance of being good as valid and the rest as invalid.

An acquisition is declared valid or invalid depending upon the following criteria:

$P_{acq} \geq$ Tolerance *and* downlink carrier in lock *results in* Acquisition declared valid

$P_{acq} <$ Tolerance *or* downlink carrier out of lock *results in* Acquisition declared invalid.

2.4 Allocation of Link Power

The equations governing the allocation of power on uplink and downlink depend on whether the range clock is sinewave or squarewave. Most often, the range clock will be sinewave but for the sake of completeness, both cases are considered here. In order to achieve economy of expression, it is advantageous to introduce the functional definitions of Table 3. Bessel functions of the first kind of order 0 and 1 are denoted $J_0(\cdot)$ and $J_1(\cdot)$.

Table 3. Definition of $\alpha(\cdot)$ and $\beta(\cdot)$

Range Clock	Command	$\alpha(\psi)$	$\beta(\psi)$
sinewave	sinewave subcarrier	$J_0\left(\sqrt{2}\psi\right)$	$\sqrt{2}\,J_1(\sqrt{2}\psi)$
squarewave	squarewave subcarrier or direct modulation	$\cos(\psi)$	$\sin(\psi)$

2.4.1 Uplink

The equations of this paragraph apply to simultaneous ranging and command using a sequential ranging signal (with sinewave or squarewave range clock) and either a command subcarrier (sinewave or squarewave) or direct modulation of the uplink carrier. The carrier suppression is

$$\left.\frac{P_C}{P_T}\right|_{\text{U/L}} = \alpha^2\left(\phi_r\right)\cdot\alpha^2\left(\phi_c\right) \tag{6}$$

The ratio of available ranging signal power to total power is

$$\left.\frac{P_R}{P_T}\right|_{\text{U/L}} = \beta^2\left(\phi_r\right)\cdot\alpha^2\left(\phi_c\right) \tag{7}$$

The ratio of available command (data) signal power to total power is

$$\left.\frac{P_D}{P_T}\right|_{\text{U/L}} = \beta^2\left(\phi_c\right)\cdot\alpha^2\left(\phi_r\right) \tag{8}$$

In these equations, ϕ_r is the uplink ranging modulation index in radians rms and ϕ_c is the command modulation index in radians rms. If no command is present, $\phi_c = 0$, $\alpha(\phi_c) = 0$, and the factor representing command modulation in Equations (6) and (7) is simply ignored.

2.4.2 Downlink

A turn-around ranging channel in the spacecraft transponder demodulates the uplink carrier, filters and amplifies the baseband signal using automatic gain control, and remodulates this signal unto the downlink carrier. The automatic gain control serves the important purpose of ensuring that the downlink carrier suppression is approximately constant, independent of received uplink signal level. A typical bandwidth for this turn-around channel is 1.5 MHz – wide enough to pass a 1 MHz range clock. Unfortunately, substantial thermal noise from the uplink also passes through this channel. In many deep space scenarios, the thermal noise dominates over the ranging signal in this turn-around channel.

The command signal on the uplink may be within the bandwidth of the ranging channel as well. When this command signal modulates the downlink carrier, it is called *command feedthrough*. In a typical deep-space scenario, the command signal is negligible compared with the noise in the wideband ranging channel. Command feedthrough is ignored in the equations appearing below. Reference 5 treats the general case where command feedthrough modulation is not negligible.

The carrier suppression is

$$\left.\frac{P_C}{P_T}\right|_{\text{D/L}} = \alpha^2\left(\theta_r\right)\cdot e^{-\theta_n^2}\cdot\cos^2\left(\theta_t\right) \tag{9}$$

The ratio of available ranging signal power to total power is

$$\left.\frac{P_R}{P_T}\right|_{\mathrm{D/L}} = \beta^2\left(\theta_r\right)\cdot e^{-\theta_n^2}\cdot\cos^2\left(\theta_t\right) \tag{10}$$

The ratio of available telemetry (data) signal power to total power is

$$\left.\frac{P_D}{P_T}\right|_{\mathrm{D/L}} = \alpha^2\left(\theta_r\right)\cdot e^{-\theta_n^2}\cdot\sin^2\left(\theta_t\right) \tag{11}$$

In these equations, θ_r is the modulation index in radians, rms that can be attributed to the ranging signal in the turn-around ranging channel, θ_n is the modulation index in radians, rms that can be attributed to thermal noise in the turn-around ranging channel, and θ_t is the telemetry modulation index.

It has been assumed that the telemetry signal is binary valued; that it is comprised of unshaped bits with a squarewave subcarrier or unshaped bits directly modulating the carrier. If the telemetry subcarrier is sinewave then the factor $\cos^2(\theta_t)$ of Equations (9) and (10) must be replaced by $J_0^2\left(\sqrt{2}\theta_t\right)$ and the factor $\sin^2(\theta_t)$ of Equation (11) must be replaced by $2J_1^2\left(\sqrt{2}\theta_t\right)$ where θ_t is the telemetry modulation index in radians, rms.

It is important to understand that the modulation indices θ_r and θ_n are effective modulation indices and that, in general, neither equals the design value θ_d of the downlink ranging modulation index (also with units radians rms). In fact, the automatic gain control circuit in the turn-around ranging channel enforces the following constraint.

$$\theta_r{}^2 + \theta_n{}^2 = \theta_d{}^2 \tag{12}$$

In other words, the total power in the turn-around ranging channel (the ranging signal power plus the noise power in the channel bandwidth) is a constant value. The effective downlink modulation indices are given by

$$\theta_r = \theta_d\cdot\sqrt{\frac{\Gamma_{\mathrm{U/L}}}{1+\Gamma_{\mathrm{U/L}}}} \tag{13}$$

$$\theta_n = \frac{\theta_d}{\sqrt{1+\Gamma_{\mathrm{U/L}}}} \tag{14}$$

where the signal-to-noise ratio in the ranging channel is

$$\Gamma_{\mathrm{U/L}} = \left.\frac{P_R}{N_0}\right|_{\mathrm{U/L}}\cdot\frac{1}{B_R} \tag{15}$$

where B_R is the turn-around ranging channel (noise-equivalent) bandwidth and $P_R/N_0\big|_{\text{U/L}}$ is

$$\left.\frac{P_R}{N_0}\right|_{\text{U/L}} = \left.\frac{P_R}{P_T}\right|_{\text{U/L}} \cdot \left.\frac{P_T}{N_0}\right|_{\text{U/L}} \tag{16}$$

where $P_T/N_0\big|_{\text{U/L}}$ is the total uplink signal power to noise spectral density ratio and $P_R/P_T\big|_{\text{U/L}}$ is the ratio of uplink ranging signal power to total power as given by Equation (7).

2.5 Uplink Spectrum

The spectrum of the uplink carrier is of concern because of the very large transmitter power used on the uplink for deep space missions. In the interest of spectral efficiency, the range clock is required to be sinewave whenever it is component 4, 5 or 6. Below are some examples of the spectrum of an uplink carrier that is phase-modulated by a sinewave range clock and also by a squarewave component multiplied by a sinewave chop component. It is assumed that ranging is the only signal that modulates the uplink carrier in all examples given here. In the more general case, where command and ranging are both present, the spectrum would be similar to that indicated below except that the ranging sidebands would be reduced by an extra suppression factor due to the presence of command and there would also be command sidebands and intermodulation products. In general, the calculation of the spectrum is quite complicated.

Since the ranging sequence consists of a set of periodic signals, the spectrum for every ranging component consists of a set of discrete spectral lines. The ratio of the power in any one discrete spectral line to the total uplink power is denoted here

$$\left.\frac{P_k}{P_T}\right|_{\text{U/L}} = \begin{cases}\text{fraction of uplink total power}\\ \text{in the discrete spectral line}\\ \text{with frequency } = f_c + kf_R\end{cases} \tag{17}$$

where f_c is the uplink carrier frequency, k is an integer harmonic number, and f_R is the frequency of the range component that presently modulates the carrier. The spectrum is symmetric about the carrier; for every discrete spectral line at $f_c + k\,f_R$, there is another of equal power at $f_c - k\,f_R$. When ranging alone modulates the carrier, the ratios of Equation (17) are subject to the conservation-of-energy law

$$\left.\frac{P_0}{P_T}\right|_{\text{U/L}} + 2\sum_{k=1}^{\infty}\left.\frac{P_k}{P_T}\right|_{\text{U/L}} = 1 \tag{18}$$

The first term in Equation (18), $P_0/P_T\big|_{\text{U/L}}$, represents the power in the residual carrier.

When the range component is a sinewave (such as the range clock, for example), the relative powers of the discrete spectral lines are given by

$$\left.\frac{P_k}{P_T}\right|_{U/L} = J_k^2\left(\sqrt{2}\phi_r\right) \tag{19}$$

where ϕ_r is the uplink ranging modulation index in radians rms and $J_k(\cdot)$ is the Bessel function of the first kind of order k. The spectrum defined by Equation (19) is illustrated in Figure 4 for the case of a 1-MHz sinewave with modulation index ϕ_r = 0.80 rad, rms, corresponding to 3 dB of carrier suppression.

The method for calculating the spectrum when the range component is multiplied by a chop component is contained in Appendix A. Some example spectra have been calculated and are reproduced below. The calculations shown here were done with account being taken of the uplink ranging filter, a low-pass Chebyshev filter with a 1.74 MHz half-power bandwidth that precedes the phase modulator in the exciter. The spectrum depends on the ratio m (a power of 2) of the (sinewave) chop component frequency to that of the (squarewave) range component. The spectrum also depends on the frequency of the chop component and the modulation index. Figures 5, 6 and 7 are for the cases m = 2, 4 and 8. For all three figures, the chop component frequency is 1 MHz and the modulation index ϕ_r = 0.80 rad rms, corresponding to 3 dB of carrier suppression. Figure 8 shows what the uplink spectrum would look like in the absence of uplink filtering; the frequencies and the modulation index are the same in Figure 8 as in Figure 7. A comparison of Figures 7 and 8, with note being taken of the different frequency scales, shows that the uplink ranging filter dramatically reduces the high-frequency content.

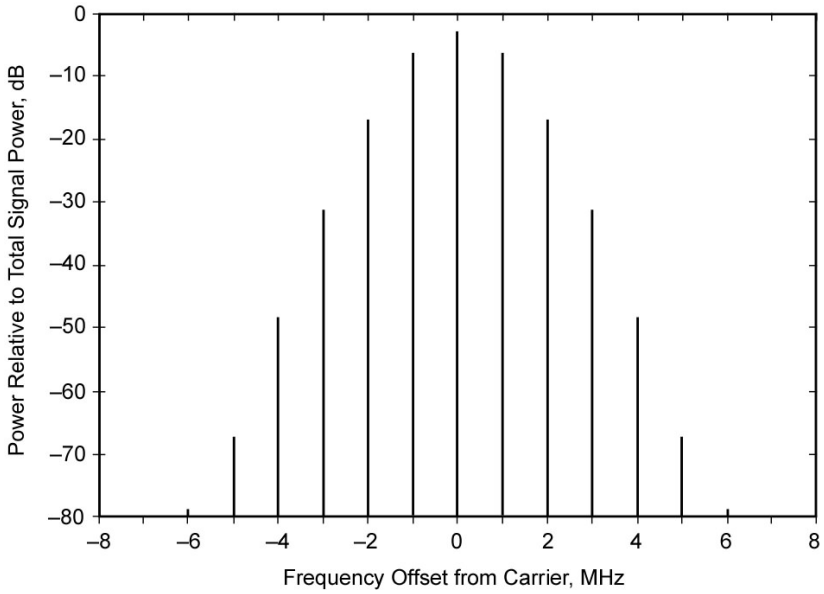

Figure 4. Spectrum for Sinewave Range Component; 1 MHz with ϕ_r = 0.80 rad rms

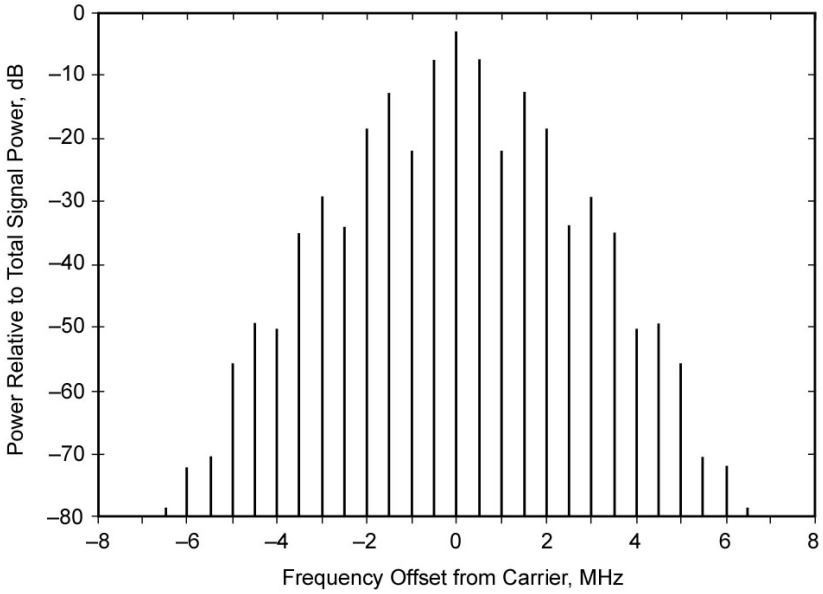

Figure 5. Spectrum With Chopping; 1-MHz, m = 2, and ϕ_r = 0.80 rad rms

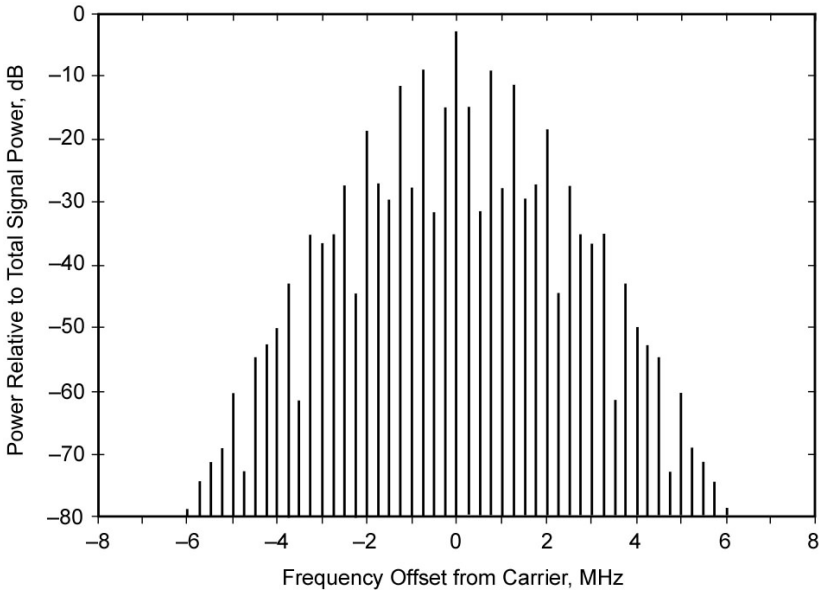

Figure 6. Spectrum With Chopping; 1-MHz, m = 4, and ϕ_r = 0.80 rad rms

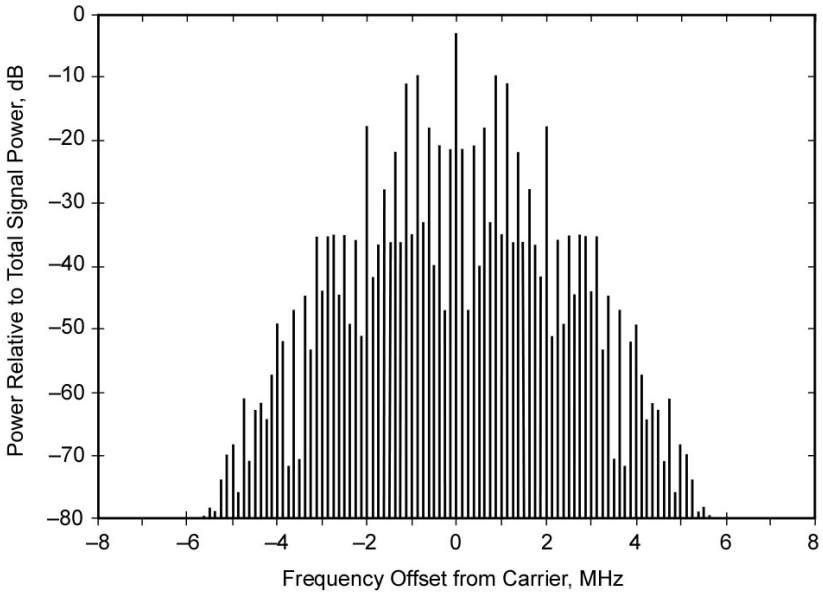

Figure 7. Spectrum With Chopping; 1-MHz, m = 8, and ϕ_r = 0.80 rad rms

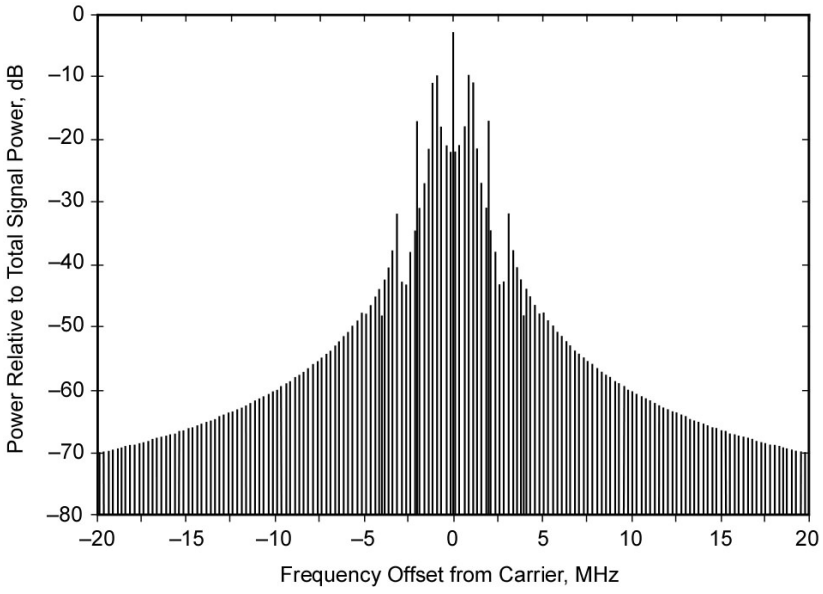

Figure 8. Unfiltered Spectrum With Chopping; Same Parameters as Figure 7

2.6 Range Measurement Performance

Thermal noise introduces an error to range measurement and also occasionally causes a range measurement to fail altogether. The error enters when the received ranging signal is correlated against the local model of the range clock. The failure to acquire a range measurement has its roots in the correlations of the received ranging signal against local models of the ambiguity-resolving components. The probability that a range measurement does not fail is called the probability of acquisition. Both the error due to thermal noise in the range clock correlation and the probability of acquisition, which is less than 1.0 due to thermal noise in the other correlations, are characterized here.

The standard deviation of two-way range measurement error σ, in meters rms (one way), due to downlink thermal noise is given by

$$\sigma = \begin{cases} \dfrac{c}{f_{RC} \cdot A_c \cdot \sqrt{32\pi^2 \cdot T_1 \cdot \left(P_R / N_0 \big|_{\mathrm{D/L}} \right)}}, & \text{sinewave range clock} \\ \dfrac{c}{f_{RC} \cdot A_c \cdot \sqrt{256 \cdot T_1 \cdot \left(P_R / N_0 \big|_{\mathrm{D/L}} \right)}}, & \text{squarewave range clock} \end{cases} \quad \text{meters, rms} \qquad (20)$$

where

c = speed of electromagnetic waves in vacuum, 299,792,500 m/s

T_1 = measurement integration time for range clock, s

f_{RC} = frequency of the range clock, Hz

A_{c} = factor that accounts for loss of correlation amplitude ($A_{\mathrm{c}} \leq 1$)

$\left. \dfrac{P_R}{N_0} \right|_{\mathrm{D/L}}$ is the downlink total signal to noise spectral density ratio, Hz, given by

$$\left. \frac{P_R}{N_0} \right|_{\mathrm{D/L}} = \left. \frac{P_R}{P_T} \right|_{\mathrm{D/L}} \cdot \left. \frac{P_T}{N_0} \right|_{\mathrm{D/L}} \qquad (21)$$

$P_T / N_0 \big|_{\mathrm{D/L}}$ is the total downlink signal power to noise spectral density ratio, and $P_R / P_T \big|_{\mathrm{D/L}}$ is the ratio of downlink ranging signal power to total power as given by Equation (10) for turn-around ranging. In the case of turn-around ranging, uplink thermal noise has an effect on measurement error through its effect on $P_R / P_T \big|_{\mathrm{D/L}}$.

The probability of acquisition is given by

$$P_{acq} = \prod_{n=n_1}^{L} P_n \tag{22}$$

where n_1 is the first ambiguity-resolving component, L is the last ambiguity-resolving component, and P_n is the probability of correctly identifying the polarity of range component n,

$$P_n = \frac{1}{2} + \frac{1}{2}\mathrm{erf}\left(\sqrt{T_2 \cdot \left.\frac{P_R}{N_0}\right|_{D/L} \cdot A_c^2}\right) \tag{23}$$

where erf(·) is the error function

$$\mathrm{erf}(y) = \frac{2}{\sqrt{\pi}} \int_0^y e^{-t^2}\, dt \tag{24}$$

and

T_2 = measurement integration time for each ambiguity-resolving component, s

A_c = factor that accounts for loss of correlation amplitude ($A_c \leq 1$)

Equations (20) and (23) are based on the assumption that the local model of the range clock has a wave shape that matches that of the received range clock. In other words, when the downlink range clock is sinewave, the local model of the range clock used in the correlation is assumed likewise to be sinewave; and when the downlink range clock is squarewave, the local model of the range clock used in the correlation is assumed likewise to be squarewave.

The factor A_c ($A_c \leq 1$) in Equations (20) and (23) accounts for the loss of correlation amplitude due to a frequency mismatch in the case of noncoherent ranging (see Paragraph 2.6.2). For two-way coherent ranging and three-way coherent ranging, there is no frequency mismatch and $A_c = 1$.

The recommended range for P_r/N_0 is –20 dB-Hz to +50 dB-Hz and range measurement performance has been validated down to –20 dB-Hz. At this low end of performance, however, the integration times are quite large. (For a given measurement accuracy, the smaller the ratio P_r/N_0, the larger the required integration time.) Although there is no upper limit on P_r/N_0, a value in excess of +50 dB-Hz is not needed. Moreover, two downlink estimators – that for the symbol signal-to-noise ratio and that for the system noise temperature – become inaccurate when P_r/N_0 is large. (See Paragraph 2.6.5.)

2.6.1 Coherent Operation

For coherent operation, the standard deviation σ of range measurement error due to thermal noise is given by Equation (20) with $A_c = 1$. (There is no frequency mismatch and no corresponding amplitude loss.) The probability of acquisition is given by Equations (22) and (23) with $A_c = 1$.

Figure 9 is derived from Equation (20) and plots the range measurement error for two-way coherent operation with $A_c = 1$ for sinewave ranging clocks of 250 kHz, 500 kHz, and 1 MHz. The abscissa is the product $T_1 \cdot P_R / N_0\big|_{D/L}$, expressed in decibels: $10\log(T_1) + 10\log\left(P_R / N_0\big|_{D/L}\right)$. A suitable value for T_1 for a given range measurement with a known $P_R / N_0\big|_{D/L}$ can be obtained from Figure 9. The minimum acceptable value for T_1 (in decibels) is found by subtracting $P_R / N_0\big|_{D/L}$ from the point on the horizontal scale corresponding to the target value of range measurement error due to thermal noise on the vertical scale. If the RTLT will vary by more than about 1 second during the tracking pass, a larger value T_1 should be selected than that just calculated by an amount equal to ΔRTLT – 1s, where ΔRTLT is the change of the RTLT over the course of the tracking pass. This increase in T_1 is needed in order to ensure an adequate overlap of the received ranging signal and the local model (see Paragraph 2.6.4.2).

Figure 10 is obtained from Equations (22) and (23) with $A_c = 1$. It plots the probability of acquisition for two-way coherent operation when using component 4 (a 1 MHz sinewave) as the range clock for range sequences having a last ambiguity-resolving component, L, of 12, 18, and 24. The abscissa is the product $T_2 \cdot P_R / N_0\big|_{D/L}$, expressed in decibels: $10\,\mathrm{Log}\left[T_2\right] + 10\,\mathrm{Log}\left[P_R / N_0\big|_{D/L}\right]$.

A suitable value for T_2 for a given range measurement with a known $P_R / N_0\big|_{D/L}$ can be obtained from Figure 10 for the case of a 1-MHz range clock. The minimum acceptable value for T_2 (in decibels) is found by subtracting $P_R / N_0\big|_{D/L}$ from the point on the horizontal scale corresponding to the target value for the probability of acquisition on the vertical scale. If the RTLT will vary by more than about 1 second during the tracking pass, then an integration time T_2 should be selected that is larger than that just calculated by an amount equal to ΔRTLT – 1s, where ΔRTLT is the change of the RTLT over the course of the tracking pass. This increase in T_2 is needed in order to ensure an adequate overlap of the received ranging signal and the local model (see Paragraph 2.6.4.2).

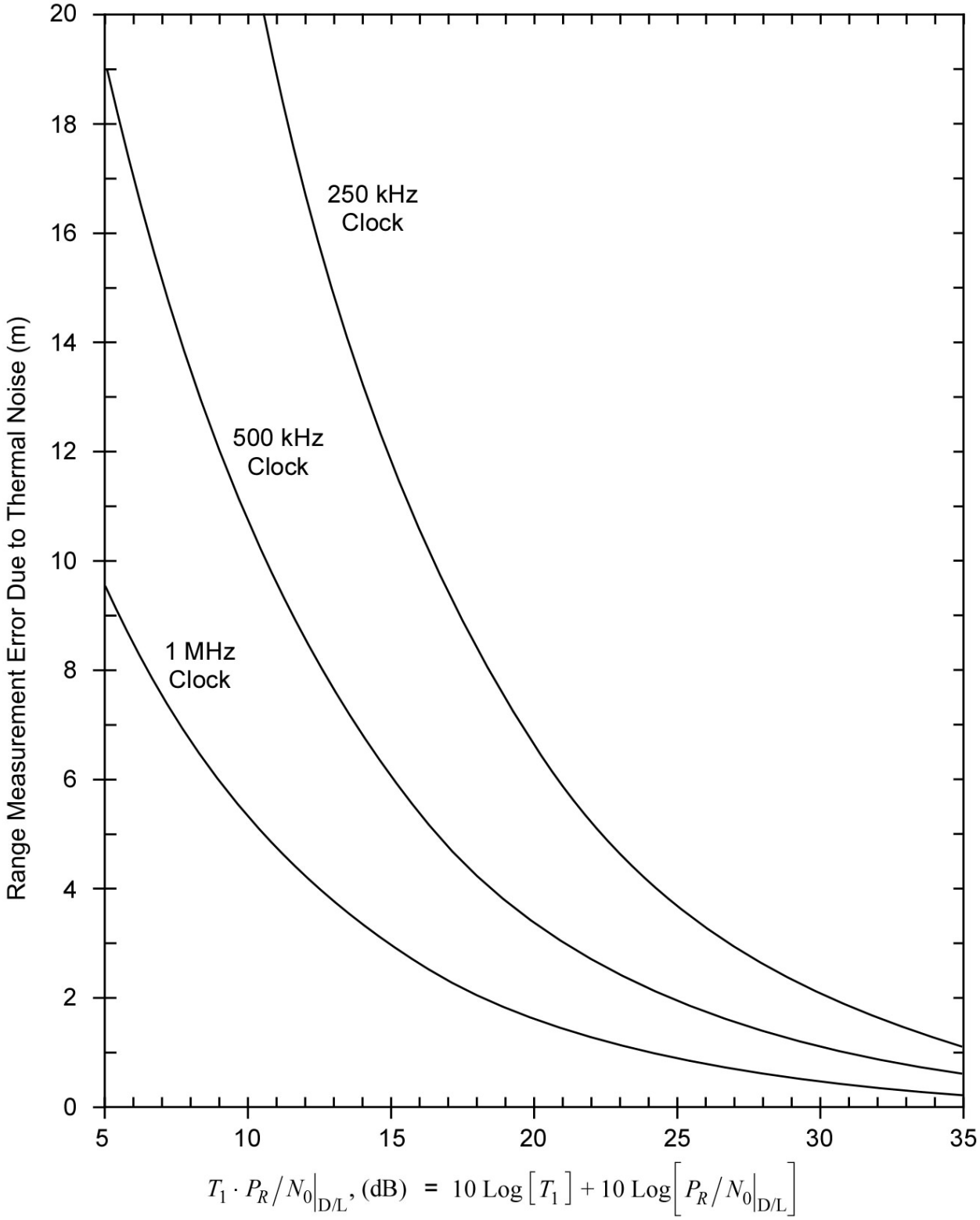

Figure 9. Two-Way Coherent Range Measurement Error for Sinewave Ranging Clocks

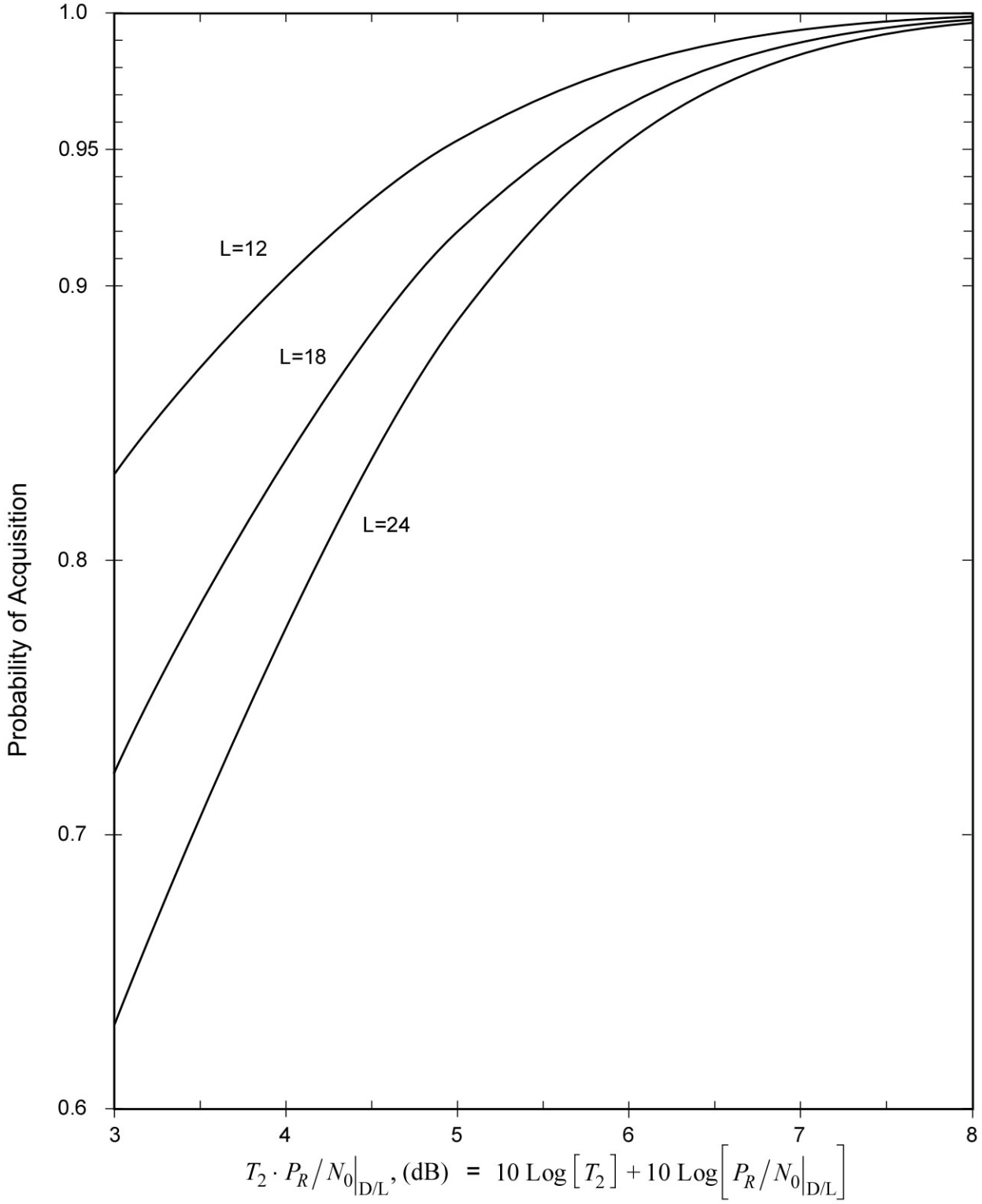

Figure 10. Probability of Acquisition for Selected Range Sequence Lengths

2.6.2 Noncoherent Operation

A two-way noncoherent ranging technique has been described in Reference 6. This technique employs a transceiver at the spacecraft rather than a transponder. As a result, the downlink carrier is not coherent with the uplink carrier and the downlink range clock is not coherent with the downlink carrier. This means that there will ordinarily be a frequency mismatch between the received downlink range clock and its local model. This mismatch can be minimized by Doppler compensation of the uplink carrier but it will not be possible, in general, to completely eliminate the frequency mismatch. Range measurement performance will not be as good as that which can be achieved with coherent ranging; however, performance will be adequate for some mission scenarios.

The frequency mismatch inherent in noncoherent ranging has two effects on performance. One is a direct contribution to range measurement error. The other is a loss of correlation amplitude that increases the thermal noise contribution to measurement error. The direct contribution is much the more important of these two effects.

The direct contribution of frequency mismatch to range measurement error is given by (see Reference 6)

$$\text{range error due to } \Delta f_{RC} = \frac{c}{4} \cdot \frac{\Delta f_{RC}}{f_{RC}} \cdot T_1 \tag{25}$$

It is worth noting that this measurement error is directly proportional to both the fractional frequency mismatch $\Delta f_{RC} / f_{RC}$ and the measurement integration time T_1. The fractional frequency error will, in general, comprise two terms: a fractional frequency error due to uncertainty in the spacecraft oscillator frequency and a fractional frequency error due to imperfect uplink Doppler predicts.

With noncoherent operation, the range error due to frequency mismatch increases with T_1 and the range error due to thermal noise decreases with T_1. Therefore, it is important to seek an optimal value for T_1, in order to get the best possible performance. Reference 6 offers guidance in this matter.

The loss of correlation amplitude is represented by the multiplicative factor A_c, where $0 < A_c < 1$. The standard deviation σ of range measurement error due to thermal noise is given by Equation (20), and the probability of acquisition (considering the effect of thermal noise) is given by Equations (22) and (23). The amplitude loss factor A_c is, for noncoherent operation, given by (see Reference 6)

$$A_c = \begin{cases} \left|\text{sinc}\left(2\Delta f_{RC} T_1\right)\right|, & \text{range clock integration} \\ \left|\text{sinc}\left(2\Delta f_{RC} T_2\right)\right|, & \text{ambiguity - resolving component integration} \end{cases} \tag{26}$$

where Δf_{RC} is the frequency mismatch between the received range clock and its local model and

$$\mathrm{sinc}(y) = \frac{\sin(\pi y)}{\pi y} \tag{27}$$

2.6.3 Three-Way Coherent Ranging

Three-way coherent ranging may be done if the RTLT is too large for two-way coherent ranging. One station transmits a ranging sequence to the spacecraft where it is received and re-transmitted. A second station receives the ranging sequence and performs the necessary correlations.

Three-way ranging yields less accurate results than two-way ranging. There are two reasons for this. First, the station delays cannot be accurately calibrated for three-way ranging. Second, the clock offset between the transmitter and receiver is imperfectly known.

Ideally, in order to get the best three-way ranging measurements, the transmitting station's one-way uplink delay and the receiving station's one-way downlink delay should be removed from the measured three-way delay. However, these one-way delays cannot be measured directly. Instead, the two-way station delay of each station is measured with the assumption that half of the delay is in the uplink equipment and the other half is in the downlink equipment. The two round-trip delays are averaged, and this average is subtracted from the round-trip phase delay to the spacecraft. This average is only as accurate as the approximation that the delay is equally distributed between the uplink and downlink at both stations.

Three-way range measurement error is often dominated by clock offset between the time reference at the transmitting and receiving stations. This clock offset can be as large as 9 μs, 3σ, and there is an additional small uncertainty of the delay between the station clock and the exciter or receiver, reference module 304 of this handbook. The largest part of the clock offset can be determined and removed from the range measurement. However, the remaining (unmodeled) clock offset translates directly into an error in three-way ranging.

2.6.4 Ranging Anomalies Related to Sequence Timing

It has been observed that there can be problems with range measurements when the integration time T_2 is very short or when the RTLT changes during a single tracking pass by an amount comparable with T_2. These anomalies, along with suggested remedies, are discussed below.

2.6.4.1 Short Integration Time T_2

If a very short integration time such as 1 or 2 s is used for T_2, the effective integration time of each ambiguity-resolving component may be significantly less that the design value of T_2. This happens if the downlink integration interval for each ambiguity-resolving component does not completely overlap the received component being integrated (see Paragraph 2.2.4.2). The difference between the design T_2 and the effective integration time will typically be a fraction of a second.

The user may suspect this problem when a very small T_2 is being used and the number of range blunder points is more than the Probability of Acquisition Tolerance should permit. The simplest solution is to increase the design T_2. It will often suffice to increase T_2 by just 1 s.

2.6.4.2 Changing RTLT

The effective integration time of each component (the range clock as well as the ambiguity-resolving components) is reduced for some range measurements if the RTLT varies significantly during a tracking pass. The estimated RTLT that is applied to ranging operations for a tracking pass is typically correct at the beginning of the pass. But if the actual RTLT moves away from this estimated value by a few seconds during the pass, a misalignment arises for range measurements occurring later in the pass. This causes the integration of any given component of measurements made later in the pass to not completely overlap the received component. The result can be an increase the range measurement error and a decrease the probability of range acquisition.

The preferred solution to the problem of a changing RTLT is to use larger values for the integration times, with due consideration for the variability of the RTLT (see Paragraph 2.6.1). With this solution, the range measurements will not degrade significantly as the tracking pass proceeds.

An alternative solution is to stop the downlink range measurements whenever the difference between the estimated RTLT and the actual RTLT exceeds some threshold and restart the downlink range measurements with an updated RTLT estimate. In order to maintain the quality of the range measurements while using the smallest possible integration times, it may be necessary to stop and restart the downlink range measurements multiple times during some tracking passes. This will be particularly true for missions having a fast-changing RTLT and small integration times. The first solution, discussed in the previous paragraph, will ordinarily be the preferred solution, due to its simplicity.

$P_R/N_0\big|_{\mathrm{D/L}}$ is estimated by the RRP during range measurements and the estimate is included in the delivered data. An accurate estimate depends on having a value for RTLT that is correct to within about 1 sec. When the RTLT changes during a tracking pass by more than about 1 sec, $P_R/N_0\big|_{\mathrm{D/L}}$ is underestimated during the later part of the tracking pass. This effect is most noticeable for large values of $P_R/N_0\big|_{\mathrm{D/L}}$. This does not have a significant effect on the range measurement error or on the probability of acquisition.

2.6.5 Interference Caused by Sequential Ranging

Sequential ranging has, on occasion, been a source of interference to conical-scan tracking and to the downlink signal power estimators. This interference is usually only an issue during early mission phase when signal-to-noise ratios are very high.

Perhaps the best-known case of such interference occurred with the Ulysses spacecraft. In that case, sequential ranging caused variations in the uplink carrier suppression, which was a problem for the conical-scan (conscan) pointing of the high-gain antenna on the Ulysses spacecraft. This is not a general problem because conscan is not used for pointing most spacecraft antennas. Furthermore, this problem for Ulysses occurred at a time when a squarewave was still being used for the 1-MHz range clock. All 1-MHz range clocks now are sinewaves, and with a sinewave range clock the variation in carrier suppression is much reduced.

Sequential ranging has also, on occasion, caused variations in the downlink residual-carrier power, which can interfere with the conscan pointing of the DSS antenna (Reference 5). This only happens when the ranging signal-to-noise ratio is large, as occurs sometimes during the early phase of a mission.

It has been observed in the early phase of some missions, shortly after launch when the signal-to-noise ratios are large, that sequential ranging can cause variations in some of the downlink signal power estimators. In particular, the symbol signal-to-noise ratio estimate may be low when a strong ranging signal is present on the downlink. This is due to the fact that the ranging signal looks like noise to the estimator. The symbol signal-to-noise ratio estimate is used as an input by the algorithm that estimates the system noise temperature. When the symbol signal-to-noise ratio estimate is low, the system noise temperature estimate is high. Both estimates have been observed to be affected by the presence of a strong ranging signal.

2.7 Range Corrections

Range measurements include delays occurring within the DSS and inside the spacecraft. These delays must be removed in order to determine the distance between a reference location on the DSS antenna and a reference location on the spacecraft antenna. The corrected delay that will be used to compute the topocentric range equals the delay measured during the ranging track minus the spacecraft delay minus the measured DSS delay plus the Z-correction, discussed below. (For DSS 27 there is also an antenna correction.) These corrections are shown schematically in Figure 11. The topocentric range then represents the distance between the DSS reference location and the spacecraft reference location. Typically, the DSS reference location (also known as the reference height) is at the intersection of the elevation and azimuth axes.

2.7.1 DSS Delay

The DSS delay is defined as the sum of the delay between the URA and range calibration coupler and the delay between range calibration coupler and the RRP. The DSS delay, defined in this way, does not account for the entire delay occurring within the station, since there is also delay between the range calibration couplers and the DSS reference location. The DSS delay is measured before each ranging track using the ranging calibration process. The measured DSS delay is also called the station delay (STDL).

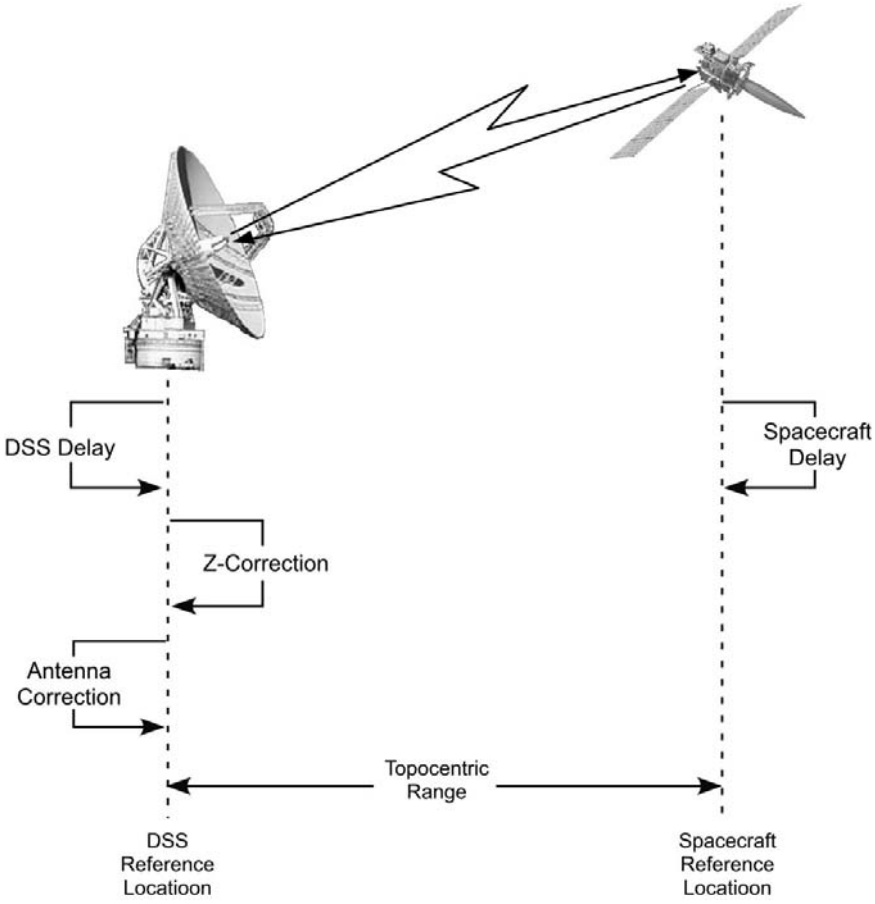

Figure 11. Correcting the Delay

The DSS delay is station and configuration dependent. It should be measured for every ranging pass. This measurement is called precal for pre-track calibration and postcal for post-track calibration. The former is done automatically at the beginning of a ranging pass; the latter is only needed when there is a change in equipment configuration during the track or precal was not performed due to a lack of time.

The DSS delay is measured by a test configuration, which approximates the actual ranging configuration. The signal is transmitted to the sky; however, before reaching the feedhorn, a sample is diverted to a test translator through a range calibration coupler. The test translator shifts the signal to the downlink frequency and reinserts the translated signal back into the received path through a range calibration coupler. The translated signal flows through the LNA to the DTT for calibration.

Figure 12 shows the signal path for a typical calibration of DSS delay when the uplink and downlink are in the same frequency band. The heavy lines identify the calibration path. When the uplink and downlink are in different bands, the downlink signal from the test translator is coupled into the receive path ahead of the LNA and as close to the feed as practical.

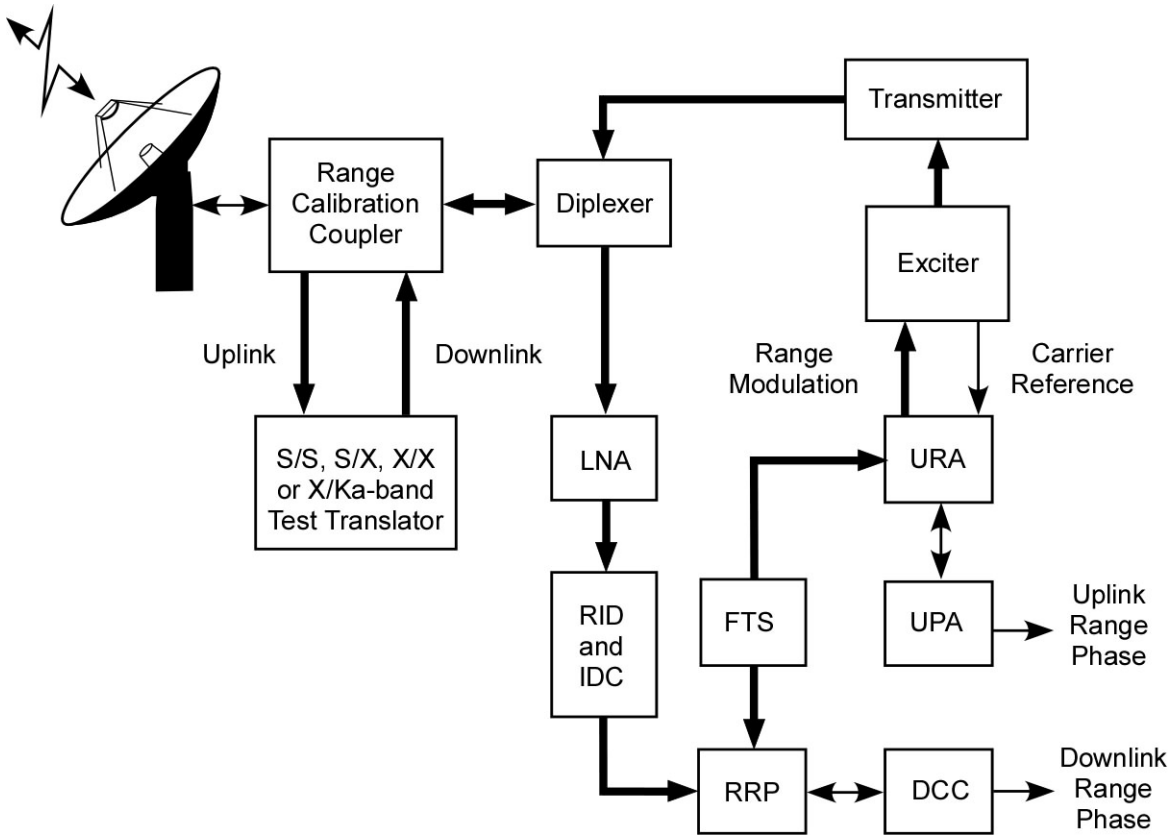

Figure 12. Typical DSS Delay Calibration

2.7.2 Z-Correction

It is not sufficient just to subtract the spacecraft delay and the measured DSS delay from the delay measured during the ranging track. With such a calculation, two discrepancies would remain (not counting the antenna correction needed for DSS 27). These discrepancies are:

1. The measured DSS delay (precal or postcal) differs from the DSS delay that is defined in Paragraph 2.7.1 in one important respect. The measured DSS delay includes the delay of the test translator and the cables connecting the test translator to the range calibration couplers. This extra delay is not part of the actual ranging path to the spacecraft during the track.

2. The DSS delay does not include the round-trip delay between range calibration couplers and the DSS reference location.

The Z-correction accounts for both of these discrepancies.

The Z-correction is the delay of the test translator and its cables minus the round-trip delay between range calibration couplers and the DSS reference location. Figure 13 relates these quantities to the physical structure of the antenna. The Z-correction is a signed quantity that can be negative when the delay between range calibration couplers and the DSS reference location is large. This is the case at the 70-m antennas and the beam waveguide antennas.

The corrected delay needed for the calculation of topocentric range is therefore the delay measured during the ranging track minus the spacecraft delay minus the measured DSS delay plus the Z-correction. For DSS 27 an antenna correction is also required.

The Z-correction is determined periodically, approximately once per year, or when there are equipment changes that affect the signal path. A current table of Z-corrections is made available for use in range measurements. The Z-correction depends on the station and the band pairing (for example, S-band uplink and X-band downlink). For an X-band downlink at some stations, the Z-correction also depends on the downlink polarization (left- or right-hand circular). Ordinarily, the Z-correction is independent of the LNA; however, at a few stations, the Z-correction even depends on this (because the location of the range calibration couplers at these stations is different for different LNAs).

In order to determine the delay of the test translator, a zero-delay device (ZDD) is connected in its place. Despite its name, the ZDD does experience delay, but the delay of this device and its connecting cables are accurately known, having been carefully measured in a laboratory. A comparison is made of the DSS delay as measured using the ZDD with that for the test translator. From this difference and the known delay of the ZDD, the delay of the test translator (and its cables) is determined.

The delay through the test translator also has a small frequency dependence. Figure 14 shows test data of the station delay as measured with a test translator as a function of channel number. Much of the variation in this figure is attributed to the test translator. Ideally, then, the Z-correction should also be a function of the channel number. However, it is impractical to measure the frequency dependence of the test translator for every configuration (station, band pairing, polarization). Therefore, the test translator delay is typically measured for just one channel (usually channel 14) for each configuration, and the Z-correction for that configuration is calculated from that measurement. During a pre-track or post-track calibration, the DSS delay is measured using the frequencies of the current track. Therefore, by ignoring the frequency dependence of the test translator delay, an absolute error is introduced to the corrected delay measurement. This error can be as large as several nanoseconds. It is should be noted, however, that for a given spacecraft using an assigned channel, the test translator delay is constant for a given configuration. Such a bias can normally be removed during the process of orbit determination.

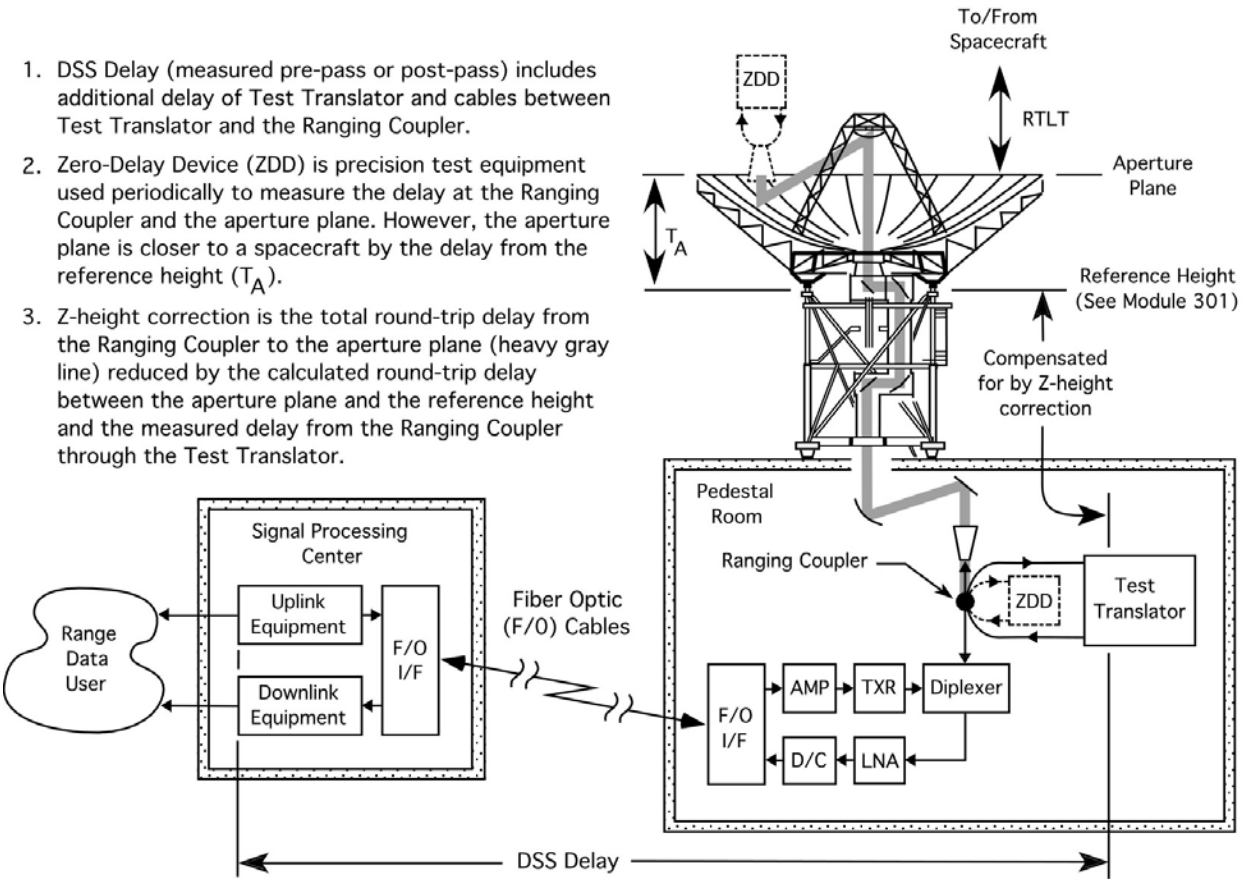

Figure 13. Measuring the Z-Correction

2.7.3 Antenna Correction

An antenna correction is required when the primary and secondary antenna axes do not intersect with the result being that the antenna reference location is not at a fixed location with respect to the Earth. The only DSN antenna where an antenna correction is necessary is the 34-m High-speed Beam Waveguide antenna, DSS 27. The antenna correction for DSS 27 can be calculated from the following expression.

$$\Delta\rho_A = 1.8288\cos\theta, \text{ m} \tag{28}$$

where θ is the antenna elevation angle.

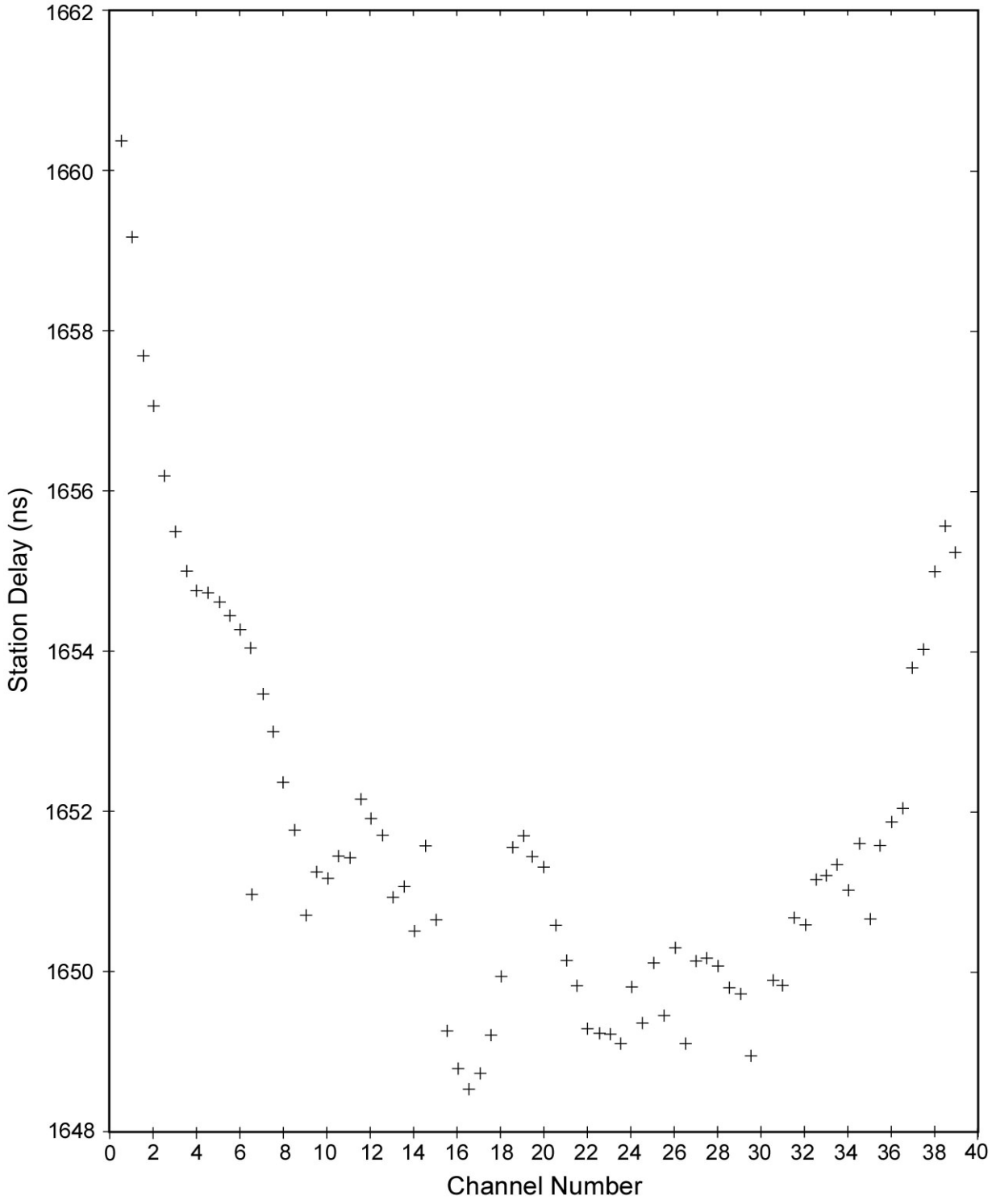

Figure 14. Station Delay as a Function of Channel Number

2.8 Ground Instrumentation Error Contribution

The ground system, the media, and the spacecraft contribute errors to range measurements. The error contributions of the media and spacecraft are outside the scope of this document and have not been included. The error due to thermal noise is discussed in Paragraph 2.6. The present paragraph estimates the error contribution from ground instrumentation, excepting thermal noise.

The round-trip one-sigma delay error of the DSN ranging system over a ranging pass has been estimated for the X-band system as 6.3 nanoseconds (about 0.95 meter one-way). The S-band one-sigma delay error has been estimated as 12.5 nanoseconds (about 1.9 meters one-way).

Table 4 provides a breakdown of long-term error contributions due to calibration and errors inherent within the equipment of the various subsystems that constitute the total DSS ground ranging system. The line item *Reserve* accounts for items that cannot be separately measured and measurement error uncertainties.

Table 4. Ground Instrumentation Range Error for the DSN Ranging System

Subsystem	X-band		S-band	
	Round-trip Delay (ns)	One-way Distance (m)	Round-trip Delay (ns)	One-way Distance (m)
FTS	1.00	0.15	1.00	0.15
Receiver	2.00	0.30	2.00	0.30
Exciter and Transmitter	1.33	0.20	5.33	0.80
Microwave and Antenna	2.33	0.35	2.33	0.35
Uplink Ranging Board	2.00	0.30	2.00	0.30
Downlink Ranging Board	2.00	0.30	2.00	0.30
Cables	1.33	0.20	1.33	0.20
Calibration	2.66	0.40	2.66	0.40
Reserve	3.33	0.50	10.0	1.50
Root Sum Square	6.33	0.95	12.47	1.87

References

1. J. B. Berner and S. H. Bryant, "Operations Comparison of Deep Space Ranging Types: Sequential Tone vs. Pseudo-Noise," *2002 IEEE Aerospace Conference*, March 9-16, 2002, Big Sky, MT.

2. J. B. Berner, S. H. Bryant, and P. W. Kinman, "Range Measurement as Practiced in the Deep Space Network," *Proceedings of the IEEE*, Vol. 95, No. 11, pp. 2202−2214, November 2007.

3. J. B. Berner and S. H. Bryant, "New Tracking Implementation in the Deep Space Network," *2nd ESA Workshop on Tracking, Telemetry and Command Systems for Space Applications*, October 29-31, 2001, Noordwijk, The Netherlands.

4. S. Bryant, "Using Digital Signal Processor Technology to Simplify Deep Space Ranging," *2001 IEEE Aerospace Conference*, March 10-17, 2001, Big Sky, MT.

5. P. W. Kinman and J. B. Berner, "Two-Way Ranging During Early Mission Phase," *2003 IEEE Aerospace Conference*, March 8-15, 2003, Big Sky, MT.

6. M. K. Reynolds, M. J. Reinhart, R. S. Bokulic, and S. H. Bryant, "A Two-Way Noncoherent Ranging Technique for Deep Space Missions," *2002 IEEE Aerospace Conference*, March 9-16, 2002, Big Sky, MT.

Appendix A

Uplink Spectrum with Chopping

This appendix describes the method for calculating the spectrum of an uplink carrier that is phase-modulated by a range component with chopping. The analysis presented here takes into account effects of the uplink ranging filter. When chopping is present, there is a lower-frequency squarewave range component multiplied by a coherently related, higher-frequency sinewave.

A key parameter is the ratio of the sinewave frequency to the squarewave frequency. This parameter, *m*, is always a power of 2. An example of how the chopped range component appears prior to filtering is shown in Figure A-1 for the case $m = 4$. One period of the chopped range component is shown.

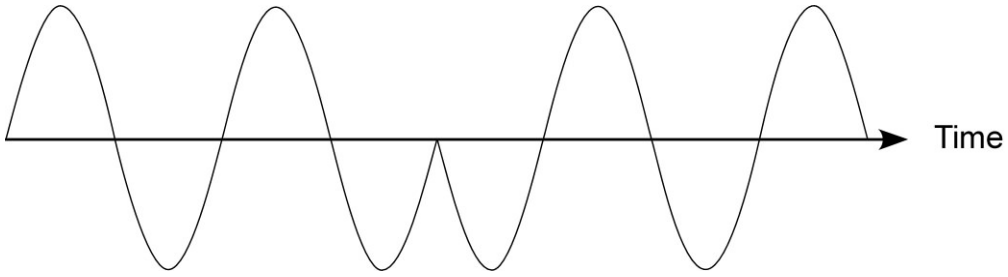

Figure A-1. Chopped range component ($m = 4$) prior to filtering

A mathematical characterization for the chopped, but as yet unfiltered, range component is now developed. This chopped signal, here denoted $x(t)$, is periodic with a fundamental frequency f_r. For any *m* of interest, the chopped range component has the same period as the squarewave from which it was derived. The reciprocal of this period is the frequency f_r of the squarewave. The periodic signal $x(t)$ may be represented with a Fourier cosine series,

$$x(t) = \sum_{\substack{k=1 \\ \text{odd}}}^{\infty} X_k \cos\left(2\pi k f_r t\right) \tag{A-1}$$

When $x(t)$ has a peak value of 1, the Fourier coefficients X_k are given by

$$X_k = \frac{4m}{\pi\left(m^2 - k^2\right)}, \; k \text{ odd} \tag{A-2}$$

This signal has half-wave symmetry, reflected in the fact that only odd harmonics are present.

The signal $x(t)$ is applied to the uplink ranging filter, a 7-pole Chebyshev low-pass filter with a 3-dB bandwidth of 1.74 MHz. For the purposes of this analysis, the filter is modeled using the following assumptions. The passband response is equiripple, and the Chebyshev filter parameter $\varepsilon = 0.11795$, corresponding to 0.03 dB of passband ripple. The cut-off frequency is 1.61 MHz. With these parameters, the 3-dB bandwidth is 1.74 MHz. The transfer function of this model for the uplink ranging filter is computed from the standard formulas of Chebyshev filter design.

The signal $y(t)$ that emerges from the filter (and that is applied to the modulator) can be represented by a Fourier series,

$$y(t) = \sum_{\substack{k=1 \\ \text{odd}}}^{\infty} Y_k \cos\left(2\pi k f_r t + \angle Y_k\right) \tag{A-3}$$

where the Y_k are complex-valued. The magnitudes $|Y_k|$ and angles $\angle Y_k$ are related to the transfer function $H(j2\pi f)$ of the uplink ranging filter and the Fourier coefficients X_k by

$$|Y_k| \exp\left(j \angle Y_k\right) = X_k \cdot H\left(2j\pi k f_r\right), \quad k \text{ odd.} \tag{A-4}$$

$y(t)$, like $x(t)$, has half-wave symmetry.

For small values of m and a 1-MHz ranging clock, the uplink ranging filter distorts the chopped range component. This is illustrated in Figure A-2 that shows one period of $y(t)$ for the $x(t)$ shown in Figure A-1 (corresponding to $m = 4$ with a 1-MHz ranging clock). The curve labeled *Input* is the unfiltered signal shown in Figure A-1, repeated here in order to make clear the effect of filtering. (The time delay introduced by the Chebyshev filter has been taken out of the $y(t)$, labeled *Output* in the figure, in order to align the two curves, making the distortion easier to visualize.)

In order to determine the spectrum of the modulated carrier, it is sufficient to consider the spectrum of its complex envelope,

$$v(t) = \sqrt{P_T}\, e^{j\theta y(t)} \tag{A-5}$$

The total power in this complex signal is P_T, and the modulation index is θ. The spectrum of the carrier with bandpass-limited modulation may be determined by simply shifting the spectrum of the complex envelope to a new center at the carrier frequency.

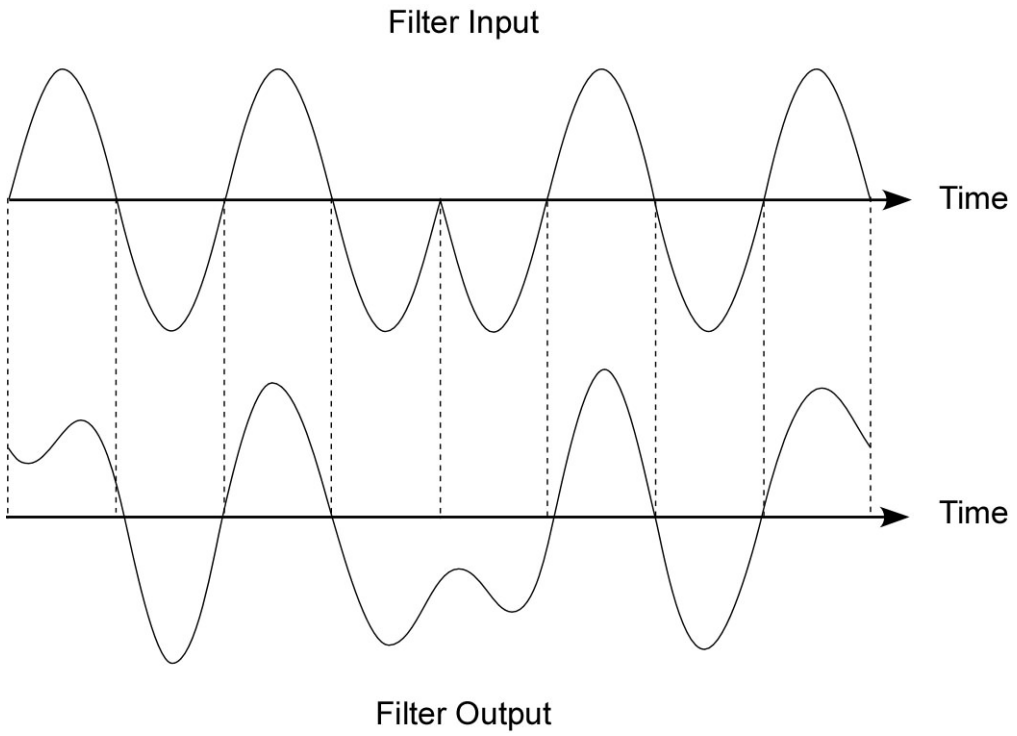

Figure A-2. Effect of filtering on chopped range component (m = 4)

Since $y(t)$ is periodic with period $T_r = 1/f_r$, $v(t)$ is also periodic with period T_r and it may therefore be expanded in a Fourier Series

$$v(t) = \sqrt{P_T} \sum_{k=-\infty}^{\infty} A_k e^{j2\pi k t/T_r} \tag{A-6}$$

The coefficients are

$$A_k = \frac{1}{T_r} \int_0^{T_r} e^{j\theta\, y(t)} e^{-j2\pi k t/T_r}\, dt \tag{A-7}$$

These coefficients must be evaluated numerically. This can be done using N samples

$$y_n = y\left(n\, T_r / N\right), \quad 0 \le n \le N-1 \tag{A-8}$$

of $y(t)$ that are uniformly spaced over T_r. Using the substitutions $t = n\, T_r$/N and $dt = T_r$/N, the coefficients of Equation A-7 can be written approximately as

$$A_k = \frac{1}{T_r} \sum_{n=0}^{N-1} e^{j\theta\, y_n} e^{-j2\pi k n/N}\, \frac{T_r}{N} \tag{A-9}$$

This can be rewritten as

$$A_k = \frac{1}{N} \cdot \mathrm{DFT}\left\{ e^{j\theta y_n} \right\} \tag{A-10}$$

where $\mathrm{DFT}\{\cdot\}$ is the Discrete Fourier Transform,

$$\mathrm{DFT}\left\{ e^{j\theta y_n} \right\} = \sum_{n=0}^{N-1} e^{j\theta y_n} e^{-j2\pi k n/N} \tag{A-11}$$

The DFT is efficiently computed by means of a Fast Fourier Transform (FFT) algorithm.

The spectrum of the carrier with bandpass-limited modulation consists of a set of discrete spectral lines, and this spectrum is symmetric about the carrier frequency. The relative power in the spectral line at frequency $f_c + kf_r$ is

$$\frac{P_k}{P_T} = \left| A_k \right|^2 \tag{A-12}$$

where f_c is the carrier frequency and P_k is the power in the k^{th} spectral line. The spectrum is symmetric about f_c; there is also a discrete spectral line with relative power P_k / P_T at the frequency $f_c - kf_r$, $k \geq 1$. The carrier suppression is given by P_C / P_T where P_C is the carrier power.